

Citation for published version:

Abd-Razak, NH, Chew, YMJ & Bird, MR 2019, 'Membrane fouling during the fractionation of phytosterols isolated from orange juice', *Food and Bioprocess Processing*, vol. 113, pp. 10-21.
<https://doi.org/10.1016/j.fbp.2018.09.005>

DOI:

[10.1016/j.fbp.2018.09.005](https://doi.org/10.1016/j.fbp.2018.09.005)

Publication date:

2019

Document Version

Peer reviewed version

[Link to publication](#)

Publisher Rights

CC BY-NC-ND

University of Bath

Alternative formats

If you require this document in an alternative format, please contact:
openaccess@bath.ac.uk

General rights

Copyright and moral rights for the publications made accessible in the public portal are retained by the authors and/or other copyright owners and it is a condition of accessing publications that users recognise and abide by the legal requirements associated with these rights.

Take down policy

If you believe that this document breaches copyright please contact us providing details, and we will remove access to the work immediately and investigate your claim.



Contents lists available at ScienceDirect

Food and Bioproducts Processing

journal homepage: www.elsevier.com/locate/fbp

Membrane fouling during the fractionation of phytosterols isolated from orange juice

Nurul Hainiza Abd-Razak^{a,b}, Y.M. John Chew^a, Michael R. Bird^{a,*}

^a Department of Chemical Engineering, University of Bath, Bath BA2 7AY, UK

^b Malaysian Rubber Board, 50450 Kuala Lumpur, Malaysia

ARTICLE INFO

Article history:

Received 30 July 2018

Received in revised form 10

September 2018

Accepted 14 September 2018

Available online xxx

Keywords:

Ultrafiltration

Phytosterols

Orange juice

Fouling

Cleaning

Nutraceuticals

ABSTRACT

The aim of this study is to isolate phytosterol compounds from orange juice using ultrafiltration (UF) flat sheet membranes (supplied by Alfa Laval) with molecular weight cut-off (MWCO) values of 10kDa fabricated from regenerated cellulose, polyethersulphone and fluoropolymer. A cross-flow filtration rig operated at a transmembrane pressure (TMP) of 0.5–2 bar, and a cross-flow velocity (CFV) of 0.5–1.5 m s⁻¹. Membrane rejection towards total phytosterols, proteins, sugars were determined along with antioxidant activity. The regenerated cellulose membrane displayed the highest permeate flux (a pseudo steady-state value of 22 L m⁻² h⁻¹), with a higher fouling index (75%) and a good separation efficiency of phytosterols (32% rejection towards phytosterols) from orange juice. Although the yield of phytosterols was relatively low (40 mg/L), there is a great potential to optimise the filtration process to produce commercially relevant amount of phytosterols. All membranes investigated displayed cleaning efficiencies of >95%.

© 2018 Institution of Chemical Engineers. Published by Elsevier B.V. All rights reserved.

1. Introduction

Plants produce diverse and complex molecules. Many of them are of high value due to their bioactivity such as phytosterols that possess cholesterol lowering (Brufau et al., 2008) and anti-oxidative properties (Wang et al., 2002). Phytosterols are also known for their anticancer effects due to their potential to inhibit cancer cell cycle progression (Shahzad et al., 2017). Increasingly, natural products are being used in many nutraceutical, pharmaceutical and food industries. Better routes for their isolation are becoming core drivers in minimising both environmental impact and operating costs. Studies are needed to recover new classes of natural products that could be of great value from agro-industrial by-products (Almanasrah et al., 2015; Conidi et al., 2017). Global market size of phytosterols was over USD 500 million in 2015 and would expand at 9% up to 2024 (Global-Market-Insight, 2016).

In 2015, the natural rubber industry in Malaysia contributed RM20 billion to the country's export earnings. This arises from the export of technically specified and speciality rubbers, latex concentrates, latex dipped goods, rubber based and rubber-wood products (MITI, 2016). The rubber tree or *Hevea brasiliensis* is key ingredient for many industrial

applications related to rubber products such as tyres, gloves and automotive devices (Kadir, 1994). The concentrated latex can be obtained by increasing the dry rubber content of *H. brasiliensis* field latex from ca. 30% to ca. 60% via centrifugation method (Devaraj and Zairossani, 2006). Centrifugation produces natural rubber serum (NRS) as a by-product that consists of primarily water and variety of non-rubber substances together with sulphuric acid with high biological oxygen demand (BOD). The by-product or waste effluent is discharged into the effluent ponds. Factories without proper maintenance of the effluent ponds face environmental problems such as air pollution and land constraints. Biological treatment system also require high operating costs to comply with the stringent environmental regulatory requirement standards set by the Malaysian Department of Environment (DOE), since water is used extensively in the rubber processing. Thus, an alternative processes for an effective rubber effluent treatment was developed using membrane separation technology to minimise waste and recover value added products from waste (Zairossani et al., 2005).

H. brasiliensis latex tapped from rubber tree contains rubber and non-rubber particles that dispersed in an aqueous serum phase (Hasma and Subramaniam, 1986; Ho et al., 1975; Hwee, 2013). Previous studies at the Malaysian Rubber Board (MRB) showed that both the sugar fraction (Devaraj and Zairossani, 2006; Mun, 1996) and the protein fraction (Aimi Izyana and Zairossani, 2011) can be successfully separated from NRS using ultrafiltration (Fig. 1). NRS contains 1–5% non-rubbers such as phytosterols, tocotrienols, lipids, carotenoid, proteins and carbohy-

* Corresponding author.

E-mail address: M.R.Bird@bath.ac.uk (M.R. Bird).

<https://doi.org/10.1016/j.fbp.2018.09.005>

0960-3085/© 2018 Institution of Chemical Engineers. Published by Elsevier B.V. All rights reserved.

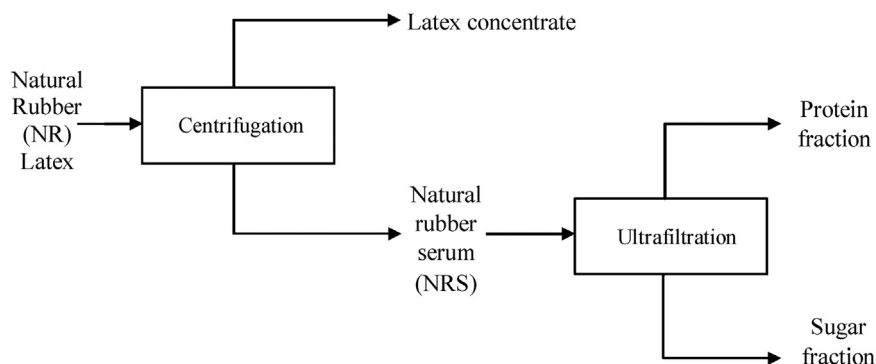


Fig. 1 – Process flow diagram of valuable product recovery from natural rubber (Devaraj and Zairossani, 2006).

Table 1 – Major components of natural rubber latex.

| Components | % (w/w) |
|---|------------|
| Water | 58.6 |
| Rubber hydrocarbons | 36.0 |
| Protein, amino acid & nitrogenous compounds | 1.7 |
| Sugar and carbohydrate | 1.6 |
| Lipids (Phytosterols) | 1.6 (0.03) |
| Ash | 0.5 |

drates (Hasma and Subramaniam, 1986; Sajari et al., 2014) as presented in Table 1. The viscosity of NRS at 20 °C was measured to be 3.5 mPa s (Muhamad, 2018). Since NRS is discharged as a waste stream from rubber processing, the NRS has a great potential to be used as an alternative source for nutraceutical compounds such as phytosterols. This project arose from the issues found in utilising the by-products of rubber processing for the recovery of high value added small non-rubber compounds from the waste. The exploitation of NRS benefits the rubber industry as it enhance raw rubber factories via integration of latex and NRS processing, and it improve competitiveness by generating value added products from rubber processing waste. Furthermore, both waste minimisation and effluent utilisation approaches are important in developing a sustainable and competitive rubber processing industry.

Nevertheless, many high value added bioactive compounds that are available have currently not been recovered and tested. A major limitation is the lack of techniques that can be used for the economical extraction and separation of these compounds. Conventional techniques such as solvent extraction, chromatography and microwave extraction consume large amounts of energy and produce considerable waste, making them costly and unsustainable (Conidi et al., 2017). This excludes them from being considered suitable for nutraceutical manufacturing. Membrane technologies such as ultrafiltration (UF) and nanofiltration (NF) offer great potential, due to their ability to separate bioactive compounds from plants and by-products of agro-industrial applications (Almanasrah et al., 2015). Ultrafiltration is a pressure-driven process that separate particles in the size range 1–100 nm (Echavarría et al., 2011). Nanofiltration is a separation process between ultrafiltration and reverse osmosis in flux and selectivity which offers relatively high permeation fluxes, high retention of molecules in the

Table 3 – Composition of orange juice.

| Components | Amount |
|---|---------------|
| Phytosterols (Jiménez-Escrig et al., 2006; Piironen et al., 2003) | 0.2–0.3 mg/ml |
| Sugar (Cobell, 2016) | ≥10° Brix |
| Protein (Cobell, 2016) | 0.7 mg/ml |

size range 100–1000 g mol⁻¹ and a much lower operational pressure than reverse osmosis (Basu and Balakrishnan, 2017). UF and NF are commonly used in pharmaceutical fractionation, water treatment and biochemical processing. The efficacy of ultrafiltration and nanofiltration in isolating steroids from wastewater (Bodzek and Dudziak, 2006; Jin et al., 2010; Nghiem et al., 2004), anthocyanin from pomegranate juice (Conidi et al., 2017), phenolic compounds from carob by-products (Almanasrah et al., 2015) and acetaminophen from pharmaceutical by-product (Basu and Balakrishnan, 2017) has been clearly demonstrated.

A model solution with similar bioactive compounds to rubber serum will be used in this study. NRS is difficult to obtain in sufficient quantities in a suitable form for experimentation due to the difficulties in transporting NRS from MRB in Malaysia to the UK. Phytosterols will be isolated from the model solution by the use of ultrafiltration technology. The same concept is thought to be applicable to natural rubber industry, potentially leading to new nutraceutical products. An extensive literature review has been performed in order to find a model solution that can replace NRS as the raw material for this project. Phytosterols or plant sterols are mostly found in vegetable oils, fruits and nuts (Jiménez-Escrig et al., 2006; Piironen et al., 2003; Plumb et al., 2011). Consequently, orange juice has been chosen as a model solution, as the type and amount of phytosterols present are similar to those present in NRS (Jiménez-Escrig et al., 2006; Piironen et al., 2003) as tabulated in Table 2. Orange juice also contains sugars (Jesus et al., 2007) and protein (Okino Delgado and Fleuri, 2016) (Table 3). In the industrial processing, fruit juice is commonly marketed in three different packaging which are frozen concentrate, fruit juice from concentrate and fruit juice not from concentrate (NFC) (Stinco et al., 2012). In this study, orange juice NFC was chosen as not from concentrate (NFC) juice can retain as much of the character of the raw fruit in which no water is added or removed. Furthermore, the pH of orange juice (pH 3.45) was found to be almost similar with pH of NRS (pH 3.56) (Muhamad, 2018).

Table 2 – Comparison of phytosterols in natural rubber serum, orange juice and kiwi juice.

| Plant | Stigmasterol (mg/kg) | Sitosterol (mg/kg) | Fucosterol (mg/kg) | Campesterol (mg/kg) | Avenasterol (mg/kg) | Stanol (mg/kg) | Other sterol (mg/kg) | Total phytosterols (mg/kg) |
|---|----------------------|--------------------|--------------------|---------------------|---------------------|----------------|----------------------|----------------------------|
| Natural rubber serum (Hasma and Subramaniam, 1986; Sajari et al., 2014) | 34 | 127 | 79 | – | – | – | – | 240 |
| Orange (Piironen et al., 2003) | 9 | 170 | – | 34 | 4 | – | 12 | 229 |
| Orange (Jiménez-Escrig et al., 2006) | 12 | 220 | – | 38 | – | 4 | 32 | 306 |
| Kiwi (Piironen et al., 2003) | 23 | 137 | – | 5 | – | 4 | 12 | 181 |
| Kiwi (Jiménez-Escrig et al., 2006) | 7 | 49 | – | 2 | – | – | 12 | 70 |

Table 4 – Characteristics of the selected membranes.

| Membrane | RC70PP | GR80PP | ETNA10PP |
|--|------------------------------------|-------------------------|------------------------------|
| Manufacturer | Alfa Laval | Alfa Laval | Alfa Laval |
| Membrane material | Regenerated cellulose acetate (RC) | Polyethersulphone (PES) | Composite fluoropolymer (FP) |
| MWCO (kDa) | 10 | 10 | 10 |
| pH operating range | 1–10 | 1–13 | 1–11 |
| pH cleaning | 1–11.5 | 1–13 | 1–11.5 |
| Operating pressure (bar) | 1–10 | 1–10 | 1–10 |
| Operating temperature (°C) | 5–60 | 5–75 | 5–60 |
| Permeability ($\text{Lm}^{-2}\text{h}^{-1}\text{bar}^{-1}$) (at 1.0 bar) | 21 | 18 | 19 |

Membrane separation techniques have been widely applied previously in fruit juices processing (Echavarría et al., 2011; Ilame and Singh, 2015). However, the literature does not report the use of ultrafiltration or nanofiltration processes for the separation of phytosterols from fruit juices. Therefore, this work will be focused on the isolation of phytosterols from orange juice via ultrafiltration technology. The performances of the selected membranes are quantified in terms of flux, rejection ratio, fouling and cleaning efficiency.

2. Materials and methods

2.1. Materials

Chloroform, acetic anhydride, sulphuric acid and methanol were sourced from Merck, UK. Stigmasterol and butylated hydroxytoluene (BHT) acquired from Sigma Aldrich, UK were used as standard. A protein assay kit was purchased from Bio-Rad, UK. The cleaning agent P3-Ultrasil 11 was purchased from Ecolab, UK. Orange juice Not From Concentrate was purchased from Cobell, Exeter, UK, and then stored in a cold room at 4 °C. The viscosity of orange juice (10°Brix) at 20 °C was recorded to be $9.24 \pm 0.03 \text{ mPa s}$. Orange juice was pre-filtered by using Amicon (Danvers, USA) pressurized feed vessel that consist of stainless steel 25 μm cartridge filter (Memtech, Swansea, UK) prior to ultrafiltration to remove the pulp. Three commercial flat-sheet membranes manufactured by Alfa Laval, Denmark, from regenerated cellulose (RC — product code RC70PP), polyethersulphone (PES — product code GR80PP) and fluoropolymer (FP — product code ETNA10PP) respectively, were tested. Their characteristics are described in Table 4 based on the manufacturer's data sheet.

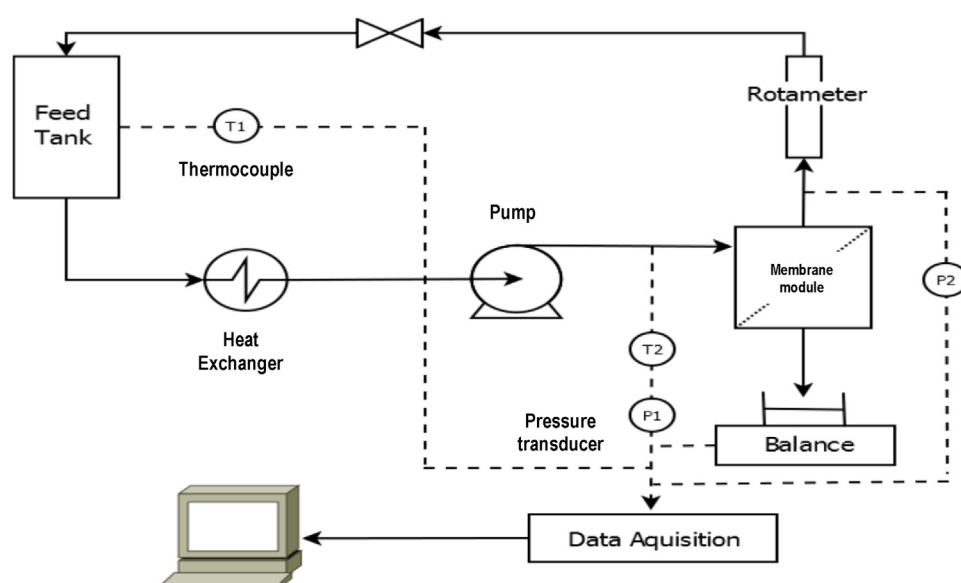
2.2. Cross-flow filtration setup

2.2.1. Cross-flow filtration system

The M10 module was connected to a pump (ECO Gearchem, NY, USA), shell and tube heat exchanger (Alfa Laval, Nakskov, Denmark), 10L conical borosilicate glass feed tank (Soham Scientific, Soham, UK) and weighing balance (Mettler Toledo, Switzerland). A schematic design of the M10 filtration system used is shown in Fig. 2. The orange juice sample (4L) was placed in the feed tank and around 1L sample was drained to the sink before the filtration to ensure that water from pure water flow has been fully removed from the system. The system had a computerized instrumentation and process control loop. Permeate mass was recorded from a weighing balance. The cross-flow velocity (CFV) was measured from the flow rate reading that was monitored by a rotameter. The pressures at the feed and retentate sides of the system were recorded by transducers in order to calculate the transmembrane pressure (TMP). A thermocouple was used to measure the temperature of the feed prior to entry into the module. All data from the balance, rotameter, transducers and thermocouple were collected by data acquisition module (model ADAM-4012, Advantech, Milpitas, USA) and then processed by Labview software (National Instruments, Austin, USA).

2.2.2. Membrane module

Ultrafiltration experiments were performed by using a cross-flow membrane filtration bench unit LabStak M10 manufactured by DSS (now Alfa Laval), Denmark. This apparatus consists of four flat sheet membranes in a module with a

**Fig. 2 – A schematic design of the M10 filtration system.**

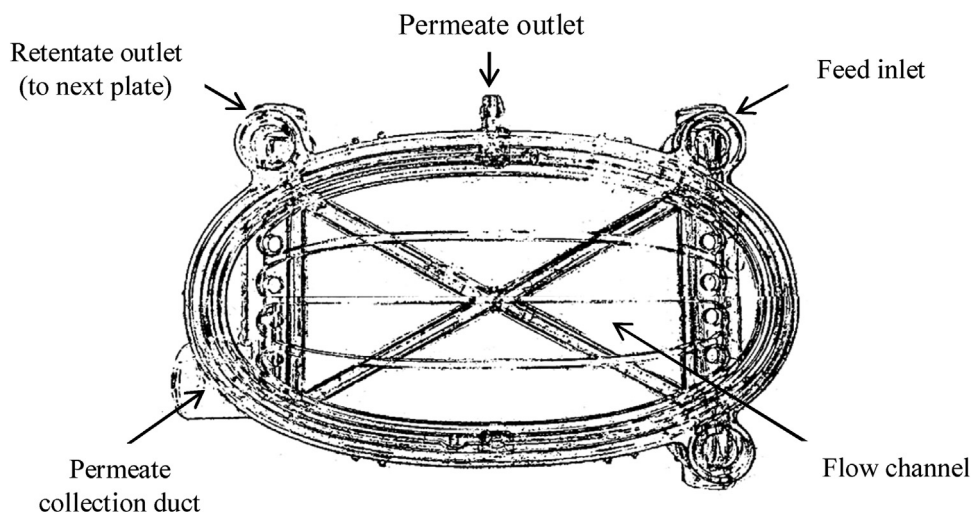


Fig. 3 – M10 module plate (Argyle et al., 2015a).

Table 5 – Cross-flow filtration cycle conditions.

| Operation stage | Duration (min) | TMP (bar) | CFV (ms^{-1}) | Temp ($^{\circ}\text{C}$) | Resistance calculated |
|-----------------------|-------------------|--------------|-----------------------------|--------------------------------|--------------------------|
| Membrane conditioning | 90 | 1.0 | 1.5 | 60 | – |
| PWF 1 | 10 | 1.0 | 1.5 | 20 | R_m |
| Filtration | 60 | 0.5–2.0 | 0.5–1.5 | 20 | R_{tot} |
| Rinse | 5 | 1.0 | 1.5 | 20 | – |
| PWF 2 | 10 | 1.0 | 1.5 | 20 | R_m |
| Cleaning | 10 | 1.0 | 1.5 | 60 | – |
| Rinse | 5 | 1.0 | 1.5 | 20 | – |
| PWF 3 | 10 | 1.0 | 1.5 | 20 | R_m |

total filtration area of 336 cm^2 . The plate-and-frame module consists of four stacked polysulfone support plates, which arranged in pairs and clamped together by two stainless steel frame. Fig. 3 illustrates the M10 module plate used in this work.

2.2.3. Cross-flow operating protocol

The cross-flow filtration cycle protocol including membrane conditioning, pure water flux (PWF) measurement, filtration, rinsing and cleaning at different time, TMP and CFV conditions (Argyle et al., 2015b) is illustrated in Table 5. The temperature of the feedstock was maintained at 20°C , and a TMP value in the range 0.5–2.0 bar was used. The CFV was in the range $0.5\text{--}1.5\text{ m s}^{-1}$. Cleaning was carried out using 0.5 wt% Ultrasil 11 (pH 11) from Henkel Ecolab, US. All membranes were coated with glycerol by the manufacturer to extend the shelf life of the membrane during storage. Therefore, new membranes were washed with water at 60°C for 90 min with 1.0 bar TMP and 1.5 ms^{-1} CFV, before filtration. This conditioning technique was established by Weis et al. (2003) to remove glycerol coating from the membrane surface. The PWF of the membrane was determined using reverse osmosis (RO) water at three different times; before filtration, after rinsing and after cleaning. The filtration time was limited to 60 min.

2.3. Characterisation of membranes

2.3.1. Contact angle measurements

Water contact angle measurements of membranes were measured via the sessile drop technique using contact angle measuring instrument (DataPhysics Instrument, Filderstadt,

Germany). This measurement represents the surface wetting characteristic of the membrane which provided information on the hydrophobicity of the membrane based on contact angle data. This procedure was repeated six times at different points on the membrane surface, taken from both sides of the drop, which were then averaged. Deionized water was used as the probe liquid.

2.3.2. Attenuated total reflectance-Fourier transform infrared (ATR-FTIR) analysis

ATR-FTIR analysis was carried out to study the surface of membrane samples. Three membrane samples were prepared; conditioned membrane, fouled membrane and cleaned membrane. The membrane samples were dried for 24 h at room temperature prior to analysis (Pihlajamäki et al., 1998). The FTIR spectra were recorded from the membrane surface using a FTIR Spectrum 100 spectrometer (Perkin Elmer, USA). Acquisition software used was Perkin Elmer Spectrum version 10.4.00.

2.3.3. Scanning electron microscope and elemental analysis

Scanning electron microscope (SEM) was used to observe the state of membrane surface at different conditions; conditioned membrane, fouled membrane and cleaned membrane. Air and vacuum-dried membranes were stuck to SEM stubs using conductive paste, followed by coating with a thin layer of gold. Then, the gold coated samples were viewed with a JEOL SEM model JSM 6480LV from Japan. The presence of elemental composition on the membrane surfaces was evaluated by energy dispersive X-ray (EDX) coupled with the SEM.

2.4. Characterisation of compounds

Feed, permeate and retentate samples from ultrafiltration experiments were collected and stored at -18°C prior to analysis. Samples were analysed for total phytosterol content, antioxidant activity, total suspended solid content, sugar and protein. These analyses were used in the calculation of rejection ratio (R) that is described in next section.

2.4.1. Total phytosterol quantification

Total phytosterol analysis was carried out using a Liebermann–Burchard (LB) based method (Mbaebie et al., 2012;

Sathishkumar and Baskar, 2014) via a spectrophotometric assay using an Ultraviolet-visible (UV-vis) Spectrophotometer (Cary 100, Agilent, USA). Absorbance was measured at 420 nm. Formation of a green colour indicated the presence of phytosterol. A calibration curve was constructed by dilution of standards of stigmasterol. The concentration of standard was performed in series dilution from 0.0625 to 1.0 mg ml⁻¹. Chloroform was used as the blank. 5 ml chloroform was added to 1 ml sample in a test tube. The mixture was vortex mixed for 1 min for nine samples. A portion of 2 ml extract was taken from that solution and mixed with 2 ml LB reagent. The LB reagent was prepared by dissolving 5 ml sulphuric acid in 50 ml acetic anhydride. The tubes were incubated for 15 min under dark condition. The total phytosterol content (TPC) was calculated using the standard photometric formula (Araújo et al., 2013; Kim and Goldberg, 1969):

$$\text{TPC} = C_s \times \frac{A_u}{A_s} \quad (1)$$

where C_s = standard concentration, A_u = Absorbance of the sample, A_s = Absorbance of the standard. All measurements were done in triplicate.

2.4.2. Antioxidant activity determination

Antioxidant activity of the samples were determined by detecting the scavenging radical of 1,1-diphenyl-2-picrylhydrazyl (DPPH) (Iqbal et al., 2015; Mbaebie et al., 2012). The assay is based on the colour change caused by reduction of DPPH radical which was determined by measuring absorbance at 517 nm (Cary 100, UV-vis Spectrophotometer, Agilent, USA). This assay was carried out as described by Iqbal et al. (2015) with some modifications. A methanolic solution of DPPH radical was freshly prepared at concentration of 0.1 mM. BHT was prepared at concentration of 0.03–0.25 mg/mL in methanol as reference. Both extract (1 ml) and BHT solution (1 ml) were mixed with 1 ml methanolic solution of DPPH. The solution was mixed vigorously and let to stand at room temperature in the dark for 30 min. Methanol was used as a control instead of extract. Absorbance at 517 nm was measured after 30 min using methanol as a blank. Antioxidant activity was expressed as percentage inhibition of the DPPH radical and was calculated according to the following equation (Mbaebie et al., 2012):

$$\text{Antioxidant activity} = \frac{(A_0 - A)}{A_0} \times 100\% \quad (2)$$

where A_0 is the absorbance of the control at $t = 0$ min and A is the absorbance of the sample at $t = 30$ min. All measurements were done in triplicate.

2.4.3. Total suspended solid quantification

Suspended solids were quantified after centrifuging 20 ml samples at 2000 rpm for 20 min using a Heraeus, Thermo Scientific centrifuge (Loughborough, UK) according to a method performed by Cassano et al. (2008). The supernatant was removed and the settled solids were dried in the oven (Townson & Mercer, Manchester, UK) at 40 °C for 48 h to ensure all water was removed. The final weight of the samples was weighed using semi-micro balance (Precisa, Newport Pagnell, UK). All measurements were done in triplicate.

2.4.4. Sugar quantification

Sugar content concentration expressed in °Brix was determined using a digital hand held refractometer (Reichert, New

York, USA). Distilled water at 0° Brix was used as a control. Samples were pipetted on the glass surface of the refractometer and Brix analysis was carried out in triplicate.

2.4.5. Protein concentration measurement

Protein concentration was determined using the Bradford assay method (Cassano et al., 2008; Kruger, 1994). The protein assay is a simple colorimetric assay for measuring total protein concentration based on the binding of the acidic dye solution Coomassie Brilliant Blue G-250 to protein at maximum absorbance from 465 to 595 nm (Bradford, 1976). The dye reagent was prepared by diluting one part of protein assay dye reagent concentrate (Bio-Rad Laboratories, Hercules, USA) with 4 parts deionized water. Bovine serum albumin (BSA) was used as standard protein and prepared at different concentration ranging from 0.2 to 1.0 mg/ml. 100 µl of standard and sample solution were pipetted into a tube and 5 ml diluted dye reagent was added. The mixed solutions were vortexed and incubated at room temperature for at least 5 min. Absorbance for the protein concentration was measured at 595 nm using UV-vis Spectrophotometer (Cary 100, Agilent, USA). The standard calibration curve was plotted for absorbance vs. protein concentration. All measurements were done in triplicate.

2.5. Evaluation of permeate flux, selectivity, fouling index and cleaning efficiency

The effectiveness of any membrane process is described in terms of permeation rate (or permeate flux) and the selectivity. The permeate flux through a membrane can be calculated as the following equation (Mulder, 1996):

$$J = \frac{\Delta P}{\mu R} \quad (3)$$

where J indicates the flux through the membrane ($\text{L m}^{-2} \text{h}^{-1}$), ΔP (bar) is the applied transmembrane pressure (TMP), μ is the viscosity and R represents the total resistance (all resistances are in m^{-1}). Selectivity is expressed as the rejection ratio (R) and calculated using this equation (Mulder, 1996):

$$R = \left(1 - \frac{C_p}{C_r}\right) \times 100\% \quad (4)$$

where C_p is the solute concentration in the permeate and C_r is the solute concentration in the retentate.

The fouling index (FI) was evaluated by comparing the pure water permeability before and after the ultrafiltration using this equation (Conidi et al., 2017):

$$FI = \left(\frac{WP_1}{WP_0}\right) \times 100\% \quad (5)$$

where WP_0 is the pure water permeability of the virgin membrane and WP_1 is the pure water permeability after the ultrafiltration. The cleaning efficiency (CE) was measured according to this equation (Conidi et al., 2017):

$$CE = \left(\frac{WP_2}{WP_0}\right) \times 100\% \quad (6)$$

where WP_2 is the pure water permeability after the cleaning.

Table 6 – Membrane surface angles of RC, PES and FP membranes.

| Membrane | Contact angle (°) | | |
|----------|-------------------|--------|---------|
| | Conditioned | Fouled | Cleaned |
| RC70PP | 11 ± 2 | 10 ± 2 | 8 ± 2 |
| GR80PP | 60 ± 2 | 40 ± 2 | 58 ± 2 |
| ETNA10PP | 65 ± 2 | 46 ± 2 | 63 ± 2 |

3. Results and discussion

3.1. Contact angle measurements

Contact angle measurements were conducted to evaluate the hydrophobicity of the membranes tested (Table 6). The conditioned RC membrane displayed a contact angle of ca. 11°, corresponding to a highly hydrophilic surface. The contact angles of the conditioned PES and FP membranes were 60° and 65° respectively. These two types of membranes tested were both considered to be moderately hydrophilic, as the contact angles measured were less than 90°. The FP membrane surface was relatively hydrophobic, which is in agreement with findings by other researcher (Nguyen et al., 2015).

Table 6 also shows the contact angles of fouled membranes. The contact angles of fouled RC, PES and FP membranes were 10 ± 2°, 40 ± 2° and 46 ± 2° respectively. These values are much lower than those for the conditioned membranes, indicating that the membranes became more hydrophilic after fouling. The contact angle measurements of fouled membranes showed the modifications of membranes hydrophobicity owing that the membrane surface is modified by surface fouling with protein-based foulants or other hydrophilic sub-micelles (Argyle et al., 2015b; Wu and Bird, 2007). After cleaning, contact angles of the cleaned surfaces increased for all three membranes. Surfaces were not returned to their original state; but instead contact angles were slightly lower than those recorded for the conditioned membranes. However, within experimental error, no difference was detected between the contact angles of the conditioned and the cleaned membranes.

3.2. Permeate flux analysis

Fig. 4 shows the time course of permeate flux for orange juice ultrafiltration at four different TMPs for all membranes. The viscosity of the permeates obtained were 6.41 ± 0.09 mPa s, 6.50 ± 0.08 mPa s and 6.43 ± 0.08 mPa s for the regenerated cellulose, polyethersulphone and fluoropolymer membranes respectively. Fig. 4(a) shows the initial permeate flux varied for RC membranes varied between 25 and 33 L m⁻² h⁻¹, and decreased gradually with filtration time. The highest initial flux was obtained at a TMP value of 1.5 bar. However, the highest steady-state flux of ca. 22 L m⁻² h⁻¹ was obtained at a TMP of 1.0 bar. For the PES membrane, the highest initial permeate flux of 30 L m⁻² h⁻¹ was seen at a TMP value of 2.0 bar (Fig. 4(b)). The flux also reduced with time. A steady-state flux value of 17 L m⁻² h⁻¹ was obtained at a TMP value of 1.0 bar. There was no change to the permeate flux observed at TMP 0.5 bar for this membrane. It can be seen from Fig. 4(c), that the trend in permeate flux for the FP membrane was similar to that recorded for the RC and PES membranes. The initial flux of the FP membrane (25 L m⁻² h⁻¹) decreased gradually over time. The permeate flux then reached a steady-state value of

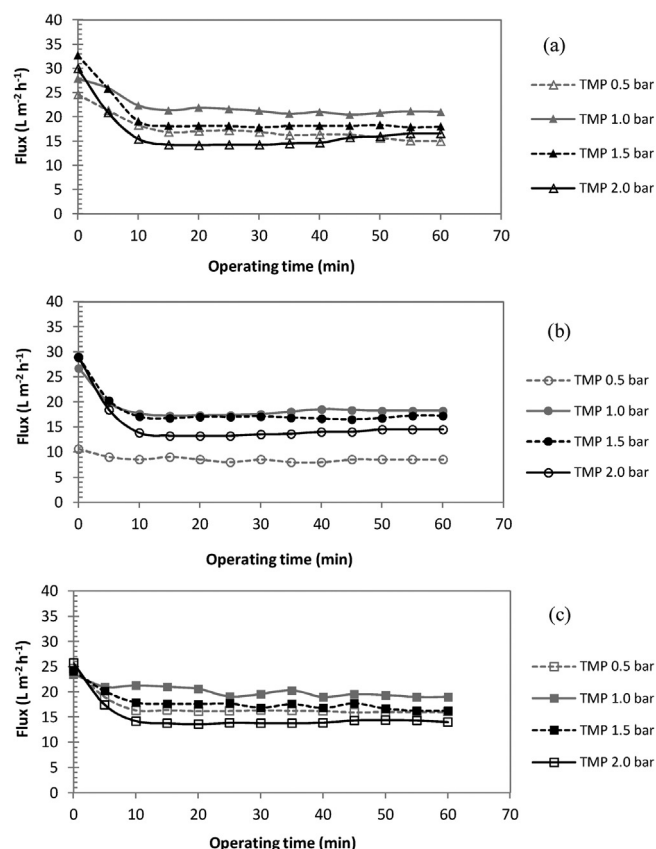


Fig. 4 – Time course of permeate flux for orange juice ultrafiltration at different pressures for a 10 kDa membrane; (a) RC (b) PES and (c) FP.

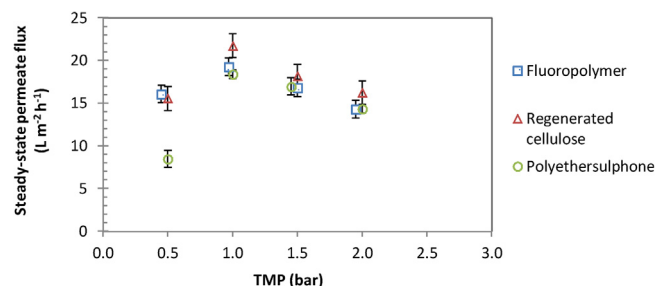


Fig. 5 – Effect of TMP upon steady-state permeate flux for orange juice UF with different membrane materials (all 10 kDa MWCO).

14–19 L m⁻² h⁻¹. Both PES and FP membranes showed lower filtration fluxes than those seen for RC. The permeate flux declined gradually with time until it reached a pseudo steady-state value. The decrease of permeate flux can be explained by the effect of fouling (Cassano et al., 2007; Conidi et al., 2017). From the values tested, a TMP of 1.0 bar was the optimal value based on the filtration performance. The highest pseudo steady-state permeate flux for all membranes were achieved at TMP of 1.0 bar. Thus, operation at a TMP of 1.0 bar has been selected for further filtration analyses.

Fig. 5 summarises the effect of increasing the TMP from 0.5 bar to 2.0 bar upon the steady-state permeate flux at 20 °C. The three membranes tested showed a similar trend and the optimal TMP for the UF of orange juice from the range tested was 1 bar. The RC membrane exhibited the highest permeate flux value of ca. 22 L m⁻² h⁻¹. However, when permeability (L m⁻² h⁻¹ bar⁻¹) is examined (Table 7), results show a different trend. The FP membrane at TMP 0.5 bar displayed the highest

Table 7 – Permeability of RC, PES and FP membranes.

| Membrane | Permeability ($\text{L m}^{-2} \text{h}^{-1} \text{bar}^{-1}$) | | | |
|----------|--|---------|---------|---------|
| | 0.5 bar | 1.0 bar | 1.5 bar | 2.0 bar |
| RC70PP | 31 ± 1 | 21 ± 2 | 12 ± 1 | 8 ± 1 |
| GR80PP | 17 ± 1 | 18 ± 1 | 11 ± 1 | 7 ± 1 |
| ETNA10PP | 32 ± 1 | 19 ± 1 | 11 ± 1 | 7 ± 1 |

permeability value. These results suggest that the permeate flux and permeability are affected not only by TMP but also by membrane material as well as by interactions between membranes and solutes. When moving above 0.5 bar, it is clear that the linear dependency of flux upon pressure is lost for the regenerated cellulose and fluoropolymer membranes. However, the polyethersulphone membrane is operating in the pressure dependant region when moving from 0.5 to 1.0 bar. Once 1.5 bar is achieved, pressure or flux linearity is lost.

3.3. Rejection of key compounds

The rejection of key compounds such as total phytosterols, sugars, proteins, total suspended solids and also the antioxidant activity was analysed for all three membranes in order to study the fractionation of phytosterols and to study the effect of membrane fouling (Fig. 6). Phytosterol compounds are hydrophobic in nature (Ostlund, 2007). Theoretically, the more hydrophobic molecules in the feed solution have a tendency to be attracted to a membrane with more hydrophobic surface (Evans et al., 2008). The RC membrane (which is highly hydrophilic) gave 32% rejection towards phytosterols (Fig. 6(a)). Nevertheless, PES (Fig. 6(b)) and FP (Fig. 6(c)) membranes exhib-

ited higher rejections towards phytosterol compounds; with rejections of 76% and 75% respectively. This observation suggests that membrane hydrophobicity is not the key factor in determining phytosterol rejection in orange juice filtration. It is also possible that the hydrophobic membrane surface is trapping more foulant than the hydrophilic membrane. Therefore, other important characteristics for rejection such as surface charge, surface roughness and membrane-foulant interaction should be explored. The antioxidant activity was expected to be directly correlated with the total phytosterol content, since phytosterols were found to have antioxidant properties (Wang et al., 2002). However, no correlation was observed between antioxidant activity and total phytosterols (Fig. 6). The rejection of antioxidant activity was in the range 10% – 23% for all selected membranes. It is possible that the antioxidant activity detected can be attributed to other chemical compounds present in orange juice, such as phenolic compounds (Stinco et al., 2012).

For protein, the rejection recorded for all membranes tested was found to be 96%–100%. Protein was especially highly rejected by the 10 kDa MWCO ultrafiltration membrane. The molecular weights of the proteins in orange juice were from 12 kDa to 71 kDa (Sass-Kiss and Sass, 2000). Thus, it would also be expected that the cake layer formed on the membrane surface would consist of a highly proteinaceous nature (Evans et al., 2008). Total suspended solids were totally removed from the orange juice, and collected as retentate in all membranes tested (100% rejection) (Fig. 6). Unsurprisingly, all of the membranes examined showed a low rejection towards sugars (5%–6%).

Table 8 shows a mass balance for the total phytosterols and proteins following RC membrane filtration. The initial volume

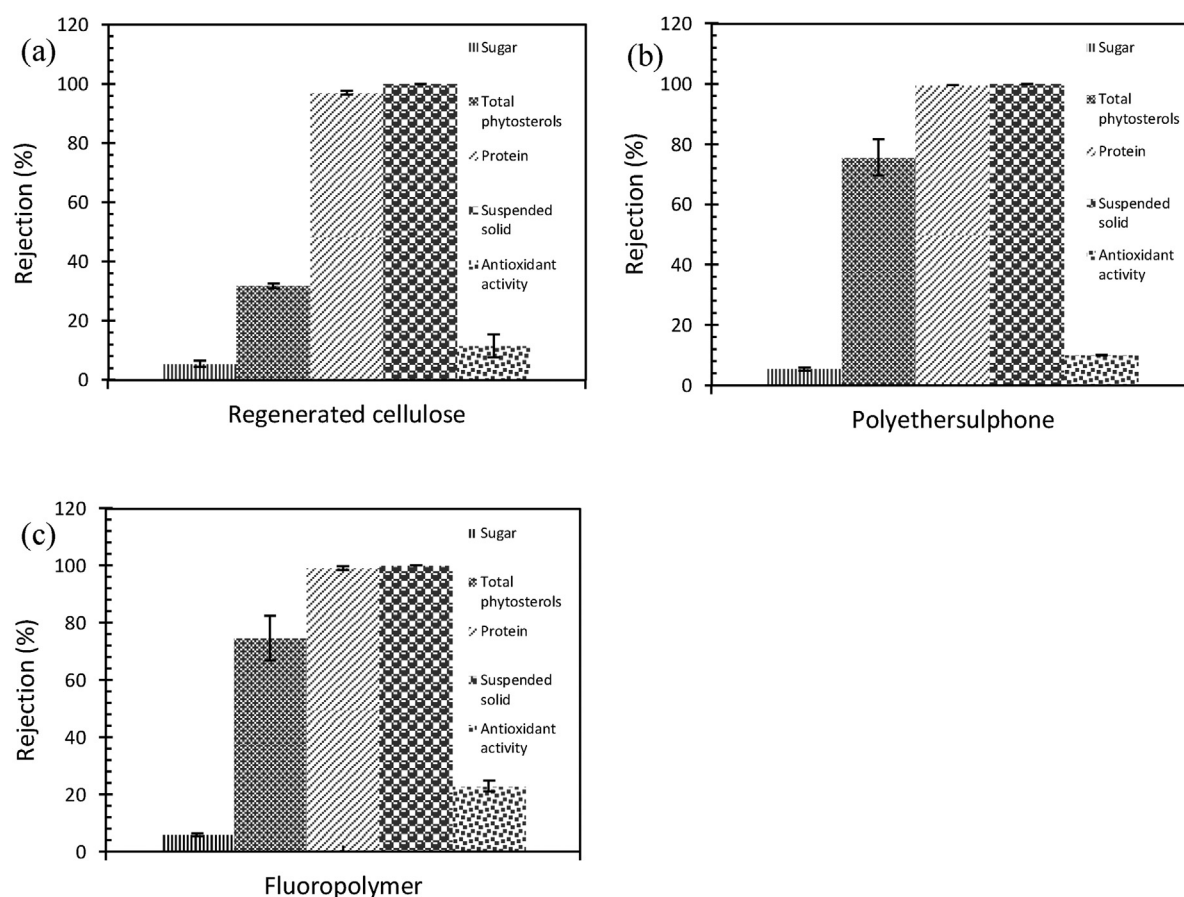
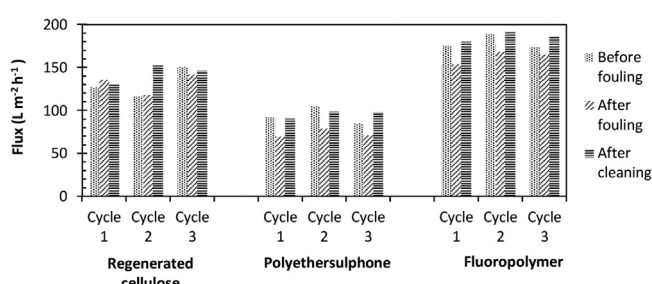


Fig. 6 – Rejection of key compounds by the three different membranes tested; (a) RC, (b) PES and (c) FP.

Table 8 – Mass balance for total phytosterols and protein by UF process of orange juice with different membranes; (a) RC (b) PES and (c) FP.

| (a) RC | Feed | Total permeate | | Final retentate | | Total (%) |
|-------------------------|------|----------------|------|-----------------|-----|-----------|
| Volume (ml) | 3000 | 850 | 28% | 2150 | 72% | 100 |
| Total phytosterols (mg) | 781 | 121 | 15% | 584 | 75% | 90 |
| Protein (mg) | 2883 | 29 | 1% | 2371 | 82% | 83 |
| (b) PES | Feed | Total permeate | | Final retentate | | Total (%) |
| Volume (ml) | 3000 | 650 | 22% | 2350 | 78% | 100 |
| Total phytosterols (mg) | 777 | 34 | 4% | 615 | 79% | 83 |
| Protein (mg) | 3121 | 7 | 0.2% | 3036 | 97% | 97 |
| (c) FP | Feed | Total permeate | | Final retentate | | Total (%) |
| Volume (ml) | 3000 | 850 | 28% | 2150 | 72% | 100 |
| Total phytosterols (mg) | 809 | 54 | 7% | 622 | 77% | 84 |
| Protein (mg) | 1499 | 3 | 0.2% | 1110 | 74% | 74 |

**Fig. 7 – Pure water fluxes of three membranes tested; RC, PES and FP.**

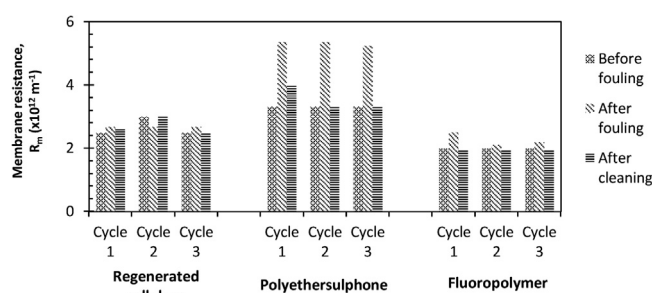
of the orange juice for the ultrafiltration was 3000 ml. Total phytosterols in feed solution were ca. 780–800 mg. The highest recovery of phytosterols in the permeate stream was achieved by using a RC membrane (albeit the amount was relatively low at 40 mg/L). In addition, the 10% loss of phytosterols in the system for RC membrane, 17% loss for PES and 16% loss for FP membranes were presumably due to the fouling effect during filtration (Cassano et al., 2008). The higher rejections seen with PES and FP in Fig. 6 are linked to a greater loss of sterols from the feed into the foulants. This is perhaps not surprising, as the surface concentrations are presumably higher, leading to an increase in the mass transfer into the foulants. The proteins detected in the retentate for all the membranes tested were found to be between 74% and 97% (Table 8). Most proteins were rejected by the 10 kDa MWCO UF membrane, since the molecular weights of protein were 12 kDa to 71 kDa. It would also be expected that the higher molecular weight compounds were rejected by smaller pore size membrane, and this increased the degree of membrane fouling (Evans et al., 2008).

3.4. Pure water flux analysis

Fig. 7 presents the pure water fluxes of selected membranes at a TMP of 1.0 bar and at 20 °C. PWF values were measured for membranes under the following conditions (i) before fouling, (ii) after fouling and (iii) after cleaning. The PES membranes displayed the lowest water flux of 69–105 L m⁻² h⁻¹, and the FP membrane gave the highest water flux of 153–191 L m⁻² h⁻¹. The highest PWF of all membranes before fouling was achieved by using FP membranes (174–189 L m⁻² h⁻¹) and the lowest PWF was shown by PES membranes (84–105 L m⁻² h⁻¹). The PWF had declined after fouling for both PES and FP mem-

Table 9 – Reduction in pure water fluxes of PES and FP membranes.

| Cycle | Flux (L m ⁻² h ⁻¹) | |
|-------|---|------------|
| | PES | FP |
| 1 | 92 to 69 | 175 to 153 |
| 2 | 105 to 79 | 189 to 168 |
| 3 | 84 to 70 | 174 to 164 |

**Fig. 8 – Variation in membrane resistance for selected membranes.**

branes, although flux declines were small, at ca. 10%. The RC membrane flux after fouling was broadly similar to that seen for the membrane before fouling. There were no significant changes in PWF through RC membranes during first and third cycle. The PWF declined for PES and FP membranes during the three fouling cycles examined (Table 9). These results indicate that the ultrafiltration process was affected by the membrane fouling phenomena. Therefore, a proper cleaning technique is needed to regenerate the membrane. In this study a commercial cleaning agent, *Ultrasil 11* (Henkel Ecolab), was used as suggested by Wu and Bird (2007).

For both PES and FP membranes, the PWF passing through the membrane after cleaning was higher than that seen after fouling. In most cases, the PWF after cleaning seen was approximately the same as that seen for the virgin membrane (Fig. 7). It is postulated that this is due to the adsorption of *Ultrasil 11* surfactant to the membrane surface (Weis et al., 2003). Given that cleaning is achieving PWF regeneration to values comparable to that virgin membrane, it can be concluded that the cleaning method using 0.5% (w/w) of *Ultrasil 11* is effective in regenerating the membrane. Fig. 8 shows the membrane resistances of the three membranes tested, under the same pressure and temperature conditions for three foul-clean cycles. It can be seen that the membrane resis-

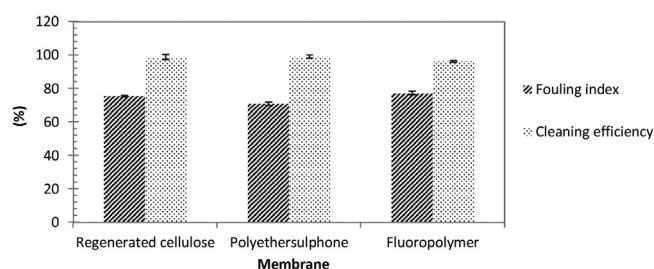


Fig. 9 – Fouling index and cleaning efficiency for RC, PES and FP membranes.

tances before filtration and after cleaning were similar for all three membranes (except for sample of PES membrane cycle 1, where differences were not large). The membrane resistances before filtration for RC, PES and FP membranes were $2.5 \times 10^{12} \text{ m}^{-1}$, $3.3 \times 10^{12} \text{ m}^{-1}$ and $2.0 \times 10^{12} \text{ m}^{-1}$ respectively. After filtration, these values increased to $2.7 \times 10^{12} \text{ m}^{-1}$, $5.3 \times 10^{12} \text{ m}^{-1}$ and $2.3 \times 10^{12} \text{ m}^{-1}$ for the RC, PES and FP membranes respectively. Following cleaning, resistances had reduced in all cases similar values to those for clean membranes.

Fig. 9 displays the fouling index and cleaning efficiency measured for all membranes tested. All measurements were carried out in triplicate. The three membranes generally displayed the almost similar fouling index. The lowest fouling index value was measured for the PES membrane (71%) followed by RC membrane (75%) and the highest fouling index was measured for FP membrane (77%). These results indicate that the ultrafiltration process was affected by the membrane fouling phenomena. In addition, all those three tested membranes (RC, PES and FP) displayed almost similar cleaning efficiencies which were 98%, 99% and 96% respectively.

3.5. Spectral analysis of membranes

FTIR spectra were collected to identify any changes in the composition of material on the membrane surfaces occurring due to fouling and cleaning processes. The intensity of IR absorption bands can be used to quantify the amount of targeted compounds deposited on the membrane (Wu and Bird, 2007). However, the foulant layers on the membrane surface were found to be too thin to generate quantitative data in this study. Thus, the FTIR spectra in the range of $4000\text{--}515 \text{ cm}^{-1}$ were used to analyse the membrane surfaces at different conditions. Fig. 10 displays the overlay results of FTIR spectra of membrane at three conditions; conditioned, fouled and cleaned condition. It was observed that all samples showed identical FTIR spectra with slightly shifted absorption bands. The RC membrane showed a higher intensity in absorbance compared to either of the PES and FP membranes. The higher intensity recorded demonstrated that more foulant was deposited on the membrane surface (Evans et al., 2008). When a membrane was fouled, the FTIR peaks of the cleaned membrane were changed in absorbance intensity. In each of the figures, fouled membranes offered higher intensity values compared to either the conditioned or cleaned membrane samples. For cleaned membranes, the intensity was reduced to values very similar intensity to those recorded for conditioned membrane. This indicates that foulant deposits present on the membrane surface were removed after cleaning.

Fig. 10(a) shows the FTIR spectrum for the RC membrane. A strong and broad band observed around $3500\text{--}3000 \text{ cm}^{-1}$ corresponds to O-H stretching vibration of hydroxyl group in

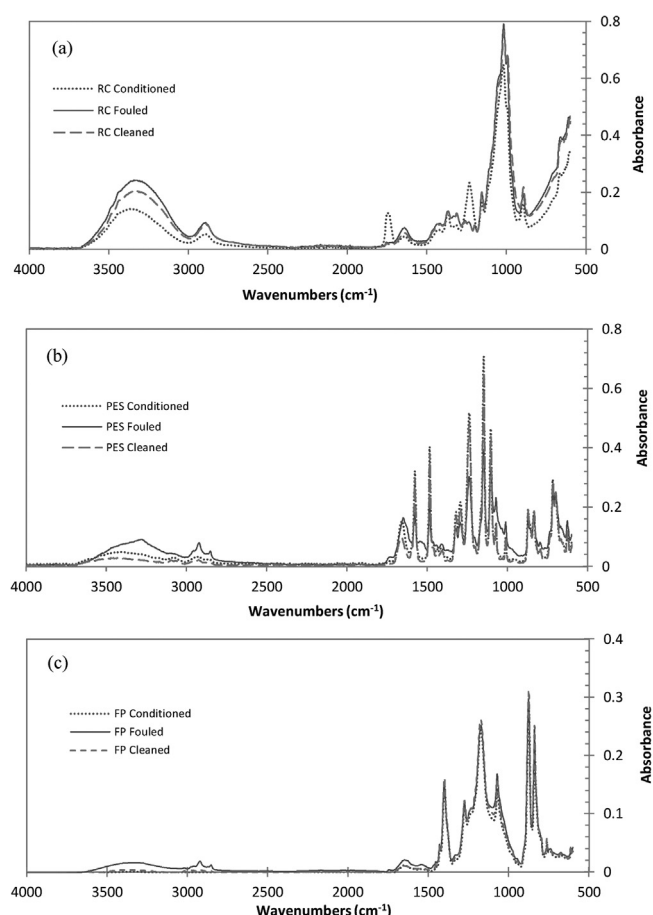


Fig. 10 – FTIR spectra of three membranes tested; (a) RC, (b) PES and (c) FP for conditioned, fouled and cleaned membranes.

the RC membrane (Madaeni and Heidary, 2011). The band at 2900 cm^{-1} is assigned to $-\text{CH}$ stretching vibration. The highest peak at 1020 cm^{-1} attribute to C-O stretching (Azuwa et al., 2015). The H-O-H bending was characterised at 1640 cm^{-1} and the band at 895 cm^{-1} is due to the C-O-C stretching (Yang et al., 2017). Fig. 10(b) illustrates the FTIR spectrum of the PES membrane. A broad peak at 3400 cm^{-1} is associated with the OH stretching. Two bands located at 2925 cm^{-1} and 2852 cm^{-1} are assigned to CH_2 asymmetric stretching band (Belfer et al., 2000). The absorption bands corresponding to the PES also observed at 1670 cm^{-1} (C=O), 1580 cm^{-1} (benzene ring C=C) and 1485 cm^{-1} (C-C bond stretching) (Zhu et al., 2015). The aromatic ether band was strongly observed at around 1240 cm^{-1} . Fig. 10(c) shows the FTIR spectrum for the FP membrane. The main characteristic of FP membrane is assigned by bands in the region of $1000\text{--}1300 \text{ cm}^{-1}$ (Evans et al., 2008). The absorption band at 1200 is due to stretching vibrations of CF_2 (Mihaly et al., 2006).

3.6. SEM analysis of membranes

The morphology of fouled deposits on membrane surfaces was evaluated scanning electron microscope (SEM). SEM was applied to monitor the differences of membrane before and after fouling and subsequent cleaning. Fig. 11 shows SEM images of 10 kDa membrane surfaces of all three membranes tested for conditioned, fouled and cleaned membrane conditions. Figs. 11(a–c) show the surfaces of RC membranes. The surface morphology of PES and FP membranes is shown in Fig. 11(d–f) and Fig. 11(g–i) respectively. Conditioned

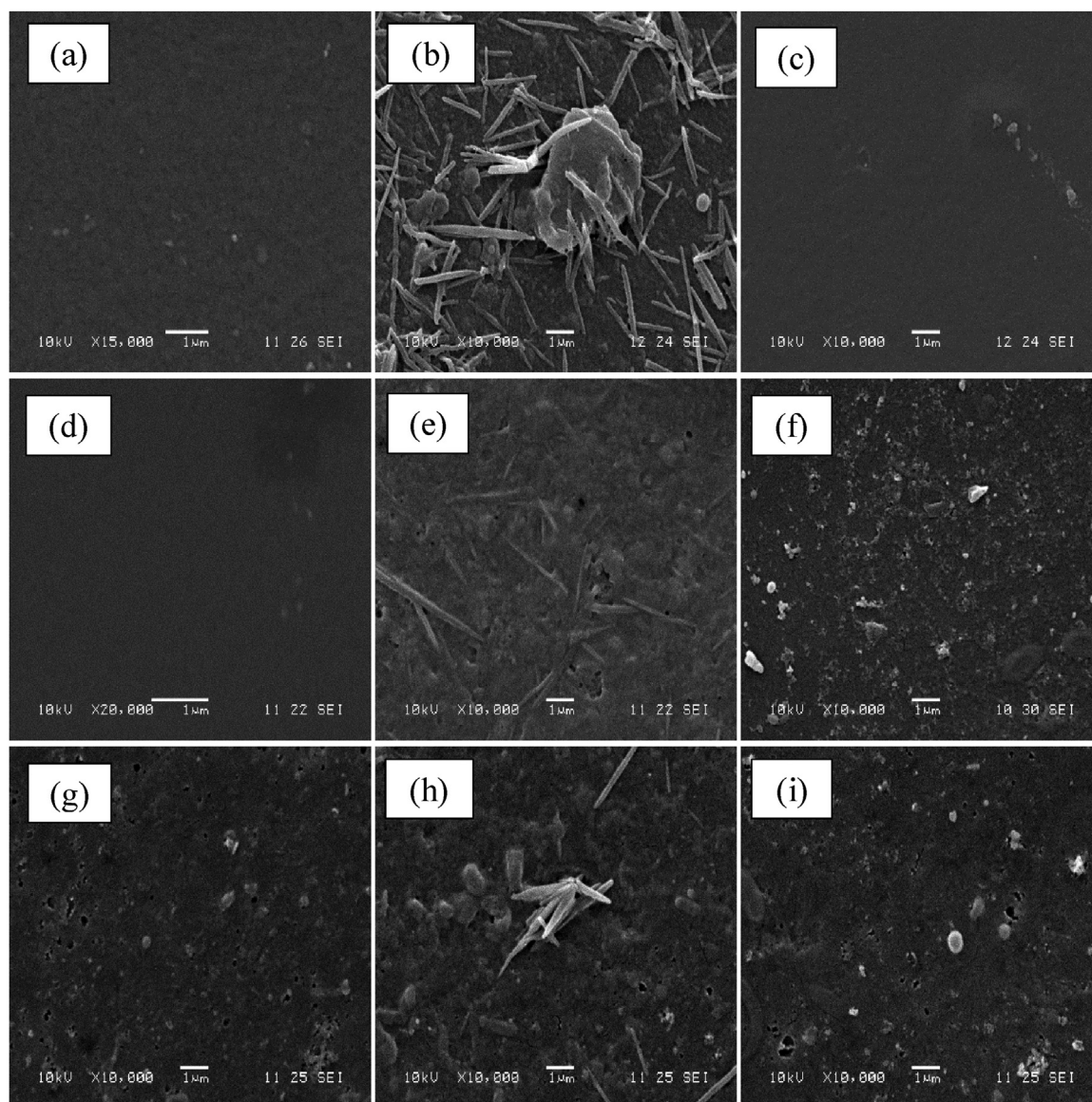


Fig. 11 – Scanning electron microscope images of 10 kD ultrafiltration membrane surfaces (a) RC conditioned membrane, (b) RC fouled membrane, (c) RC cleaned membrane, (d) PES conditioned membrane, (e) PES fouled membrane, (f) PES cleaned membrane, (g) FP conditioned membrane, (h) FP fouled membrane and (i) FP cleaned membrane.

membrane of all three membranes appeared to have clean membrane surfaces. The deposits could be seen very clearly on the fouled membrane surfaces. The fouled membrane was completely covered with a fouling layer (Fig. 11(b), (e) and (h)). This may suggest that a cake layer may dominate the filtration properties of the membrane and this is in agreement with the flux data and rejection results. The deposits could be the rejected protein and other compounds such as phytosterols that retain on the membrane surface. After the cleaning steps, cleaned membranes demonstrate that the cleaning process was able to remove most of the fouled deposits and regenerate the membrane. This observation indicates that the membranes are effectively cleaned after the 0.5% Ultrasil 11 protocol was applied.

The elemental examinations were carried out by EDX analysis that coupled with the SEM. The EDX results confirm the presence of Ca and Fe on the membrane surfaces after fouling. According to the literature (Navarro et al., 2011; Schmutzer et al., 2016), orange juice contains elements such as Ca and Fe. The EDX analyses on the surface of conditioned and cleaned membranes were also carried out. The RC membranes showed

the presence of C and O elements. These results are not surprising, given that the membranes were fabricated from cellulose (Li et al., 2014). Three elements (C, O and S) were observed on the PES membranes, consistent with membranes made of polyethersulphone (Basri et al., 2011). FP membranes showed the existence of C and F elements. It can be seen that the elements exist in conditioned membranes were similar to the elements in cleaned membranes. This result correlates well with the SEM analysis that suggests the membranes were regenerated effectively after the cleaning protocol was applied.

3.7. Process development

Now that the effectiveness of membranes as a technology for phytosterol concentration has been established, future work on process development will look to build on this foundation by maximising rejection of sterols and minimising fouling. Since the yield of total phytosterols compounds that are fractionated by using 10 kDa ultrafiltration membrane was relatively low, there is the potential for process optimisation.

From the three membrane types tested, hydrophilic RC membranes gave the best rejection ratio of phytosterol (32%). Thus, an experimental programme will be developed to introduce hybrid membrane filtration using the regenerated cellulose membrane. Membranes with larger MWCO will be tested in order to remove the proteins and transmit the sterols. Then, a second membrane step with a small MWCO can reject the sterols and transmit the sugars. Diafiltration may also be applied in concentrating the targeted compounds.

4. Conclusions

The isolation of phytosterols from orange juice has been investigated using three types of 10 kDa molecular weight cut-off (MWCO) ultrafiltration (UF) membranes made from regenerated cellulose (RC), polyethersulphone (PES) and fluoropolymer (FP). For the PES and FP membranes, there was a significant concentration of sterols in the retentate, with sterol rejections of ca. 80%. However, feed volumes used were small (3L) and ca. 20% of the sterols originally present in the feed formed part of the fouling layer on the membrane surface. Permeate fluxes decreased gradually with operating time until they reached steady-state values. The optimum TMP condition tested was found to be 1 bar based on the highest pseudo steady-state permeate flux for all membranes that were achieved at TMP of 1.0 bar. The RC membrane exhibited the highest permeate flux seen, which was ca. $22 \text{ L m}^{-2} \text{ h}^{-1}$. Hydrophilic RC gave a 32% phytosterol rejection ratio. PES and FP (more hydrophobic membranes) demonstrated higher rejections towards phytosterol compounds (76% and 75% respectively). This could be due to the fact that the membrane hydrophobicity was not the decisive factor for phytosterols rejection in orange juice. There was no correlation observed between antioxidant activity and total phytosterol content. Proteins were 100% rejected by the 10 kDa membrane, and sugar has been readily recovered in the permeate (although diafiltration was not applied). Fouling lead to a 10% reduction of phytosterols in the system recorded for RC membrane filtration, and a ca. 20% reduction was recorded for the PES and FP membranes. Permeate water fluxes after cleaning increased to levels similar to those seen for membranes before fouling. Of the membranes tested, the RC membrane displayed the highest permeate flux, the highest transmission of phytosterols from orange juice, and the highest fouling index and cleaning efficiency, when compared to the PES and FP membranes. Ultrasil 11 (0.5 wt%) was found to be effective in regenerating all membranes tested.

Acknowledgements

We wish to thank Professor Frank Lipnizki, University of Lund, for arranging for the donation of the membranes used in this study through Alfa Laval, Denmark. The financial support provided by the Malaysian Rubber Board (MRB) is gratefully acknowledged.

References

- Aimi Izyana, I., Zairossani, M.N., 2011. [Effect of spray drying on protein content of natural rubber Serum](#). *IJUM Eng. J.* 12, 61–65.
- Almanasrah, M., Brazinha, C., Kallioinen, M., Duarte, L.C., Roseiro, L.B., Bogel-Lukasik, R., Carvalheiro, F., Mänttari, M., Crespo, J.G., 2015. [Nanofiltration and reverse osmosis as a platform for production of natural botanic extracts: The case study of carob by-products](#). *Sep. Purif. Technol.* 149, 389–397.
- Araújo, L.B.D.C., Silva, S.L., Galvão, M.A.M., Ferreira, M.R.A., Araújo, E.L., Randau, K.P., Soares, L.A.L., 2013. [Total phytosterol content in drug materials and extracts from roots of *Acanthospermum hispidum* by UV-vis spectrophotometry](#). *Rev. Bras. Farmacogn.* 23, 736–742.
- Argyle, I.S., Pihlajamäki, A., Bird, M.R., 2015a. [Ultrafiltration of black tea using diafiltration to recover valuable components](#). *Desalin. Water Treat.* 53, 1532–1546.
- Argyle, I.S., Pihlajamäki, A., Bird, M.R., 2015b. [Black tea liquor ultrafiltration: Effect of ethanol pre-treatment upon fouling and cleaning characteristics](#). *Food Bioprod. Process.* 93, 289–297.
- Azuwa, M.M., Salleh, W.N.W., Juhana, J., Ismail, A.F., Muhazri, A.M., Munira, J.S., 2015. [Feasibility of recycled newspaper as cellulose source for regenerated cellulose membrane fabrication](#). *J. Appl. Polym. Sci.*, 132.
- Basri, H., Ismail, A.F., Aziz, M., 2011. [Polyethersulfone \(PES\)–silver composite UF membrane: Effect of silver loading and PVP molecular weight on membrane morphology and antibacterial activity](#). *Desalination* 273, 72–80.
- Basu, S., Balakrishnan, M., 2017. [Polyamide thin film composite membranes containing ZIF-8 for the separation of pharmaceutical compounds from aqueous streams](#). *Sep. Purif. Technol.* 179, 118–125.
- Belfer, S., Fainchtein, R., Purinson, Y., Kedem, O., 2000. [Surface characterization by FTIR-ATR spectroscopy of polyethersulfone membranes-unmodified: modified and protein fouled](#). *J. Membr. Sci.* 172, 113–124.
- Bodzek, M., Dudziak, M., 2006. [Elimination of steroidal sex hormones by conventional water treatment and membrane processes](#). *Desalination* 198, 24–32.
- Bradford, M.M., 1976. [A rapid and sensitive method for the quantitation of microgram quantities of protein utilizing the principle of protein-dye binding](#). *Anal. Biochem.* 72, 248–254.
- Brufau, G., Canela, M.A., Rafecas, M., 2008. [Phytosterols: physiologic and metabolic aspects related to cholesterol-lowering properties](#). *Nutr. Res.* 28, 217–225.
- Cassano, A., Donato, L., Conidi, C., Drioli, E., 2008. [Recovery of bioactive compounds in kiwifruit juice by ultrafiltration](#). *Innovative Food Sci. Emerg. Technol.* 9, 556–562.
- Cassano, A., Marchio, M., Drioli, E., 2007. [Clarification of blood orange juice by ultrafiltration: analyses of operating parameters: membrane fouling and juice quality](#). *Desalination* 212, 15–27.
- Cobell, 2016. [Orange Juice Not From Concentrate \(NFC\)](#). Cobell, Exeter, United Kingdom.
- Conidi, C., Cassano, A., Caiazzo, F., Drioli, E., 2017. [Separation and purification of phenolic compounds from pomegranate juice by ultrafiltration and nanofiltration membranes](#). *J. Food Eng.* 195, 1–13.
- Devaraj, V., Zairossani, M.N., 2006. [Zero Discharge and Value Added Products from NR Skim Latex Processing Malaysian Rubber Technology Developments](#). Malaysian Rubber Board, Kuala Lumpur, pp. 19–21.
- Echavarría, A.P., Torras, C., Pagán, J., Ibarz, A., 2011. [Fruit juice processing and membrane technology application](#). *Food Eng. Rev.* 3, 136–158.
- Evans, P.J., Bird, M.R., Pihlajamäki, A., Nyström, M., 2008. [The influence of hydrophobicity: roughness and charge upon ultrafiltration membranes for black tea liquor clarification](#). *J. Membr. Sci.* 313, 250–262.
- Global-Market-Insight, 2016. [Phytosterols Market Size By Product \(Beta-Sitosterol, Campesterol, Stigmasterol\), By Application \(Pharmaceuticals, Food ingredients, Cosmetics\), Regional Outlook \(U.S., Canada, Mexico, Germany, UK, France, Italy, Russia, Poland, China, India, Japan, Indonesia, Malaysia, Thailand, Australia, Brazil, South Africa, Saudi Arabia, UAE\), Growth Potential, Price Trend, Competitive Market Share & Forecast, 2016–2024](#). Global Market Insights, Inc., Delaware USA. <https://www.gminsights.com/industry-analysis/phytosterols-market/>. (Accessed 22 July 2018).

- Hasma, H., Subramaniam, A., 1986. *Composition of Lipids in Latex of Hevea Brasiliensis Clone RRIM 501*. *Journal of Natural Rubber Research* 1, 30–40.
- Hwee, E.A., 2013. Non rubbers and abnormal groups in natural rubber. In: Thomas, S., Chan, C.H., Pothan, L.A., Rajisha, K.R., Maria, H.J. (Eds.), *Natural Rubber Materials*. The Royal Society of Chemistry, United Kingdom, pp. 53–72.
- Ilame, S.A., Singh, V.S., 2015. Application of membrane separation in fruit and vegetable juice processing: a review. *Crit. Rev. Food Sci. Nutr.* 55, 964–987.
- Iqbal, E., Salim, K.A., Lim, L.B.L., 2015. Phytochemical screening: total phenolics and antioxidant activities of bark and leaf extracts of *Goniothalamus velutinus* (Airy Shaw) from Brunei Darussalam. *J. King Saud Univ. Sci.* 27, 224–232.
- Jesus, D.F., Leite, M.F., Silva, L.F.M., Modesta, R.D., Matta, V.M., Cabral, L.M.C., 2007. Orange (*Citrus sinensis*) juice concentration by reverse osmosis. *J. Food Eng.* 81, 287–291.
- Jiménez-Escrig, A., Santos-Hidalgo, A.B., Saura-Calixto, F., 2006. Common Sources and Estimated Intake of Plant Sterols in the Spanish Diet. *J. Agric. Food Chem.* 54, 3462–3471.
- Jin, X., Hu, J., Ong, S.L., 2010. Removal of natural hormone estrone from secondary effluents using nanofiltration and reverse osmosis. *Water Res.* 44, 638–648.
- Kadir, A.A.S.A., 1994. *Advances in natural rubber production*. *Rubber Chem. Technol.* 67, 537–548.
- Kim, E., Goldberg, M., 1969. Serum cholesterol assay using a stable Liebermann-Burchard reagent. *Clin. Chem.* 15, 1171–1179.
- Kruger, N.J., 1994. The Bradford method for protein quantitation. *Methods Mol. Biol.* 32, 9–15.
- Li, R., Liu, L., Yang, F., 2014. Removal of aqueous Hg(II) and Cr(VI) using phytic acid doped polyaniline/cellulose acetate composite membrane. *J. Hazard. Mater.* 280, 20–30.
- Madaeni, S.S., Heidary, F., 2011. Improving separation capability of regenerated cellulose ultrafiltration membrane by surface modification. *Appl. Surf. Sci.* 257, 4870–4876.
- Mbaebie, B.O., Edeoga, H.O., Afolayan, A.J., 2012. Phytochemical analysis and antioxidants activities of aqueous stem bark extract of *Schotia latifolia* Jacq. *Asian Pac. J. Trop. Biomed.* 2, 118–124.
- Mihaly, J., Sterkel, S., Ortner, H.M., Kocsis, L., Hajba, L., Furdyga, É., Minka, J., 2006. FTIR and FT-Raman spectroscopic study on polymer based high pressure digestion vessels. *Croat. Chem. Acta* 79, 497–501.
- MITI, 2016. *Ministry of International Trade and Industry (MITI) Report 2015*. Ministry of International Trade and Industry, Kuala Lumpur, Malaysia.
- Muhamad, A.K., 2018. *Personal Correspondance*. Malaysian Rubber Board, Kuala Lumpur, Malaysia.
- Mulder, M., 1996. *Basic Principles of Membrane Technology*, 2nd ed. Kluwer Academic Publishers, The Netherlands.
- Mun, L.C., 1996. *Quebrachitol — A Carbohydrate Extract from Hevea Latex*. Rubber Research Institute of Malaysia, Kuala Lumpur.
- Navarro, P., Perez-Lopez, A.J., Mercader, M.T., Carbonell-Barrachina, A.A., Gabaldon, J.A., 2011. Antioxidant activity, color, carotenoids composition, minerals, vitamin C and sensory quality of organic and conventional mandarin juice: cv. Orogrande. *Food Sci. Technol. Int.* 17, 241–248.
- Nghiem, L.D., Schäfer, A.I., Elimelech, M., 2004. Removal of Natural Hormones by Nanofiltration Membranes: Measurement Modeling, and Mechanisms. *Environ. Sci. Technol.* 38, 1888–1896.
- Nguyen, L.A.T., Schwarze, M., Schomäcker, R., 2015. Adsorption of non-ionic surfactant from aqueous solution onto various ultrafiltration membranes. *J. Membr. Sci.* 493, 120–133.
- Okino Delgado, C.H., Fleuri, L.F., 2016. Orange and mango by-products: Agro-industrial waste as source of bioactive compounds and botanical versus commercial description—a review. *Food Rev. Int.* 32, 1–14.
- Ostlund Jr., R.E., 2007. Phytosterols: cholesterol absorption and healthy diets. *Lipids* 42, 41–45.
- Pihlajamäki, A., Väisänen, P., Nyström, M., 1998. Characterization of clean and fouled polymeric ultrafiltration membranes by Fourier transform IR spectroscopy—attenuated total reflection. *Colloids Surf., A Physicochem. Eng. Aspects* 138, 323–333.
- Piironen, V., Toivo, J., Puupponen-Pimiä, R., Lampi, A.-M., 2003. Plant sterols in vegetables: fruits and berries. *J. Sci. Food Agric.* 83, 330–337.
- Plumb, J.A., Rhodes, M.J.C., Lampi, A.M., Buchgraber, M., Kroon, P.A., 2011. Phytosterols in plant foods: Exploring contents: data distribution and aggregated values using an online bioactives database. *J. Food Compos. Anal.* 24, 1024–1031.
- Sajari, R., Abd-Razak, N.H., Yusof, F., Arif, S.A.M., Perkins, M., Yeang, H.Y., 2014. Improved efficiency of tocotrienol extraction from fresh and processed latex. *J. Rubber Res.* 17, 245–260.
- Sass-Kiss, A., Sass, M., 2000. Immunoanalytical method for quality control of orange juice products. *J. Agric. Food Chem.* 48, 4027–4031.
- Sathishkumar, T., Baskar, R., 2014. Screening and quantification of phytochemicals in the leaves and flowers in the leaves and flowers of *Tabernaemontana heyneana* Wall. *Indian J. Nat. Prod. and Res.* 5, 237–243.
- Schmutzer, G.R., Dehelean, A., Magdas, D.A., Cristea, G., Voica, C., 2016. Determination of stable isotopes minerals, and volatile organic compounds in Romanian orange juice. *Anal. Lett.* 49, 2644–2658.
- Shahzad, N., Khan, W., Md, S., Ali, A., Saluja, S.S., Sharma, S., Al-Allaf, F.A., Abduljaleel, Z., Ibrahim, I.A.A., Abdel-Wahab, A.F., Afify, M.A., Al-Ghamdi, S.S., 2017. Phytosterols as a natural anticancer agent: Current status and future perspective. *Biomed. Pharmacother.* 88, 786–794.
- Stinco, C.M., Fernández-Vázquez, R., Escudero-Gilete, M.L., Heredia, F.J., Meléndez-Martínez, A.J., Vicario, I.M., 2012. Effect of orange juice's processing on the color particle size, and bioaccessibility of carotenoids. *J. Agric. Food Chem.* 60, 1447–1455.
- Wang, T., Hicks, K.B., Moreau, R., 2002. Antioxidant activity of phytosterols oryzanol, and other phytosterol conjugates. *J. Am. Oil Chem. Soc.* 79, 1201–1206.
- Weis, A., Bird, M.R., Nyström, M., 2003. The chemical cleaning of polymeric UF membranes fouled with spent sulphite liquor over multiple operational cycles. *J. Membr. Sci.* 216, 67–79.
- Wu, D., Bird, M.R., 2007. The fouling and cleaning of ultrafiltration membranes during the filtration of model tea component solutions. *J. Food Process Eng.* 30, 293–323.
- Yang, E., Zakaria, S., Chia, C.H., Rosenau, T., 2017. Bifunctional Regenerated cellulose membrane containing TiO₂ nanoparticles for absorption and photocatalytic decomposition. *Sains Malaysiana* 46, 637–644.
- Zairossani, M.N., Devaraj, V., Zin, A.K.M., Zaid, I., 2005. Modern approaches towards effective effluent treatment. In: *Rubber Planters Conference 2005*, Malaysian Rubber Board, Kuala Lumpur, Malaysia.
- Zhu, S., Shi, M., Zhao, S., Wang, Z., Wang, J., Wang, S., 2015. Preparation and characterization of a polyethersulfone/polyaniline nanocomposite membrane for ultrafiltration and as a substrate for a gas separation membrane. *RSC Adv.* 5, 27211–27223.